ISSN 1330-3651 (Print), ISSN 1848-6339 (Online)
https://doi.org/10.17559/TV-20190704215843
Original scientific paper

Determination of Characteristics of a Laminated Torsion Bar Spring by Using Correction Coefficients in Respect to Clamping Conditions

Vinko MOČILNIK, Jožef PREDAN, Nenad GUBELJAK

Abstract: The laminated torsion bar is used for many mechanical purposes where a large angle with decreasing or increasing torque is necessary. The design of laminated torsion bar relates to dissipation of energy by friction between laminae, number of laminae and clamp conditions at the end of bar. The paper presents theoretical, experimental and numerical analysis of a laminated torsion bar with different numbers of laminae. Results show that in the design of a laminated torsion bar it is necessary to consider correction coefficients with respect to the geometry of laminae and the clamping conditions on both sides of the laminated torsion bar. In this paper the correction coefficients are experimentally determined. We present the procedure for determination of correction parameters for the calculation of the laminated torsion spring characteristics with a relatively large ratio of width and thickness, ($h/b > 7$) for low rigidity of the individual lamella.

Keywords: laminated torsion bar; rectangular section; spring characteristics; torsion; windup

1 INTRODUCTION

This article presents the approach for determining the correction parameters for calculating the spring characteristics of the spring package with a relatively large aspect ratio $h/b > 7$.

The paper presents theoretical, experimental and numerical analysis of a laminated torsion bar with different numbers of laminae. This is reflected in a decrease in the load capacity, or slightly lower characteristics of the spring package. Due to the successful operation of the spring package, it must be released in the suspension so that the minimum relative movement between the lamellae is possible, which requires a certain clearance when installing the package.

Laminated torsion bars are widely used for different purposes in the car industry e.g. for truck tilt cab, vehicle suspension, suspending cannon breach mechanisms, pre-load at flaps, etc. The cross-section of the laminated torsion bar consists of several laminae with a rectangular cross section, made of spring steel such as 52CrMoV4. During the loading of a laminated torsion bar, when both sides of the bar are fixed, non-reversible movement appears. In order to keep the same loading characteristics, the so-called torsion rate of at least one side of the laminated torsion bar needs to be released. Additionally, the surfaces of the laminae are lubricated in order to reduce the friction between them. In general, in text books SAE International (2000) [1], the analytical and empirical model for the dimensioning of a laminated torsion bar assumes that several rectangular cross sections rotate during the elastic windup angle in the torsional direction. In SAE International [1] the η^2 and η^3 are used as Saint-Venant's stress coefficient and stiffness coefficient, respectively, for aspect ratios of width to thickness (h/b) between 2 to 7.

Swanson (1998) [2] analysed a torsion bar with a thin, laminated rectangular cross - section, based on an existing solution in literature for torsion of a laminated bar with a general rectangular cross-section, made from AS4/3501-6 carbon/epoxy fibre composite material. He stated that the speciality of thin sections is important, as it can be applied to a laminated bar with general open cross-sections. Figures show that aspect ratio has a strong effect on the lamination sequence and consequently on the accuracy of the results.

Danao & Cabrera (2007) [3] presented a torsion problem of a rectangular prismatic bar, using the Saint-Venant's windup function method and analytic solution to the twisting torque and non - vanishing shear stresses. The approximate model and the mathematical formulation presented in their paper allow for conducting uniform torsion analysis of rectangular solid cross section. Easy and quickly calculable expressions of maximum shearing stresses for midwide and mid-narrow sides of the rectangular cross–section have been derived. There are also several papers and text books which deal with the same problem, [4-10].

The mathematical models found in literature [11] for the dimensioning of the laminated torsion bar take into account the torsional windup of a multiple rectangular cross-section consisting of several laminae, without respect to the spacing between the laminae due to relative movement, which leads to the small differences in elastic spring characteristics between the calculation and the actual situation.

The goal of this paper is to find the influence of clamping at the end of a laminated torsion bar on its torsion rate *kt*. An approach for the determination of coefficients applied to a laminated torsion bar with constant lengths and a single cross-section is presented, but differently clamping the bar ends. The analytically, numerically and experimentally obtained results are compared with the SAE International text book. An experiment was performed by measuring the elastic torsion rate (the windup and the torque) of the spring bar with different number of laminae (from 1 up to 9 laminae) in a laminated torsion bar. The calculated torque and the measured one were compared with numerical modelling results in order to confirm the empirically determined correction coefficients. The correction coefficients were obtained as the ratio between the measured and analytical calculated torque. By comparing the calculated and measured torques, we obtained the correction coefficients as the ratio between the measured and analytical predicted result. The correction coefficients are expressed as a function of the windup angle, and the number of spring laminae in laminated torsion bar.

2 PURE TORSION OF A BAR WITH A TIGHT RECTANGULAR CROSS-SECTION

The torsion of a bar with an arbitrary cross-section was solved by Saint-Venant in 1855. This analytical solution is directly applicable to some simple cross-section shapes subjected to torsion, such as a circle, an ellipse and a rectangle.

Fig. 1 shows undeformed and deformed prismatic bar of a rectangular cross section $b \times h$, loaded with torsion, placed in a rectangular Cartesian coordinate system. The bar is loaded with torque T in the direction of coordinate axis z, as shown in Fig. 1.

During the acting torque, the bar is elastically deformed by the windup angle. The problem of torsion of a prismatic bar (Fig. 1) of an arbitrary cross-section can be solved using the following differential equation:

$$\Delta\Phi(x,y) = \frac{\partial^2\Phi}{\partial x^2} + \frac{\partial^2\Phi}{\partial y^2} = \mathrm{C} \tag{1}$$

where Φ is Prandtl's wrapping function, and C is a constant. The following assumptions of the boundary conditions should be taken into account:

$\sigma_x = \sigma_y = \sigma_z = 0$, $\tau_{xy} = 0$, $\tau_{zx} = \tau_{xz} \neq 0$ and $\tau_{zy} = \tau_{yz} \neq 0$.

The solution of the Eq. (1) for an arbitrary shape of cross-section presents the following function:

$$\Phi(x,y) = \frac{\mathrm{C}}{2} \cdot \left[x^2 - \frac{b^2}{4} + \psi(x,y) \right] \tag{2}$$

where $\psi(x,y)$ is a harmonic function. Since $\Delta\Phi = \mathrm{C}$, it must be the case that $\Delta\psi = 0$ and at the boundary $\Phi(B) = 0$, [10]. The dependence between the windup function and the torque T is:

$$T = 2 \cdot \int_A \Phi(x,y) \cdot \mathrm{d}A \tag{3}$$

where $A = b \times h$ is a cross-section of a torsion loaded prismatic bar.

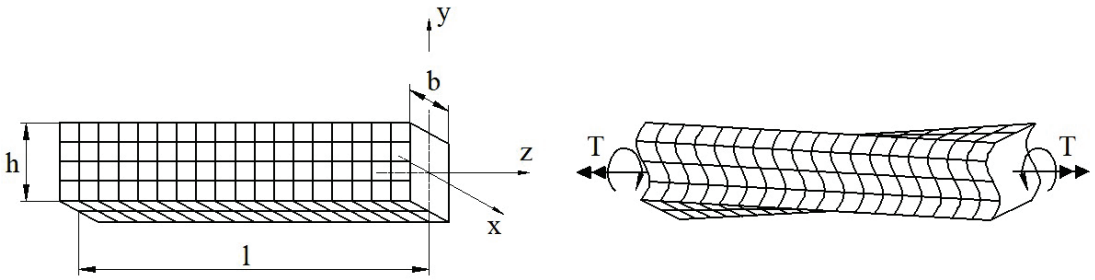

Figure 1 Undeformed and deformed prismatic bar with rectangular cross-section, subjected to torsion

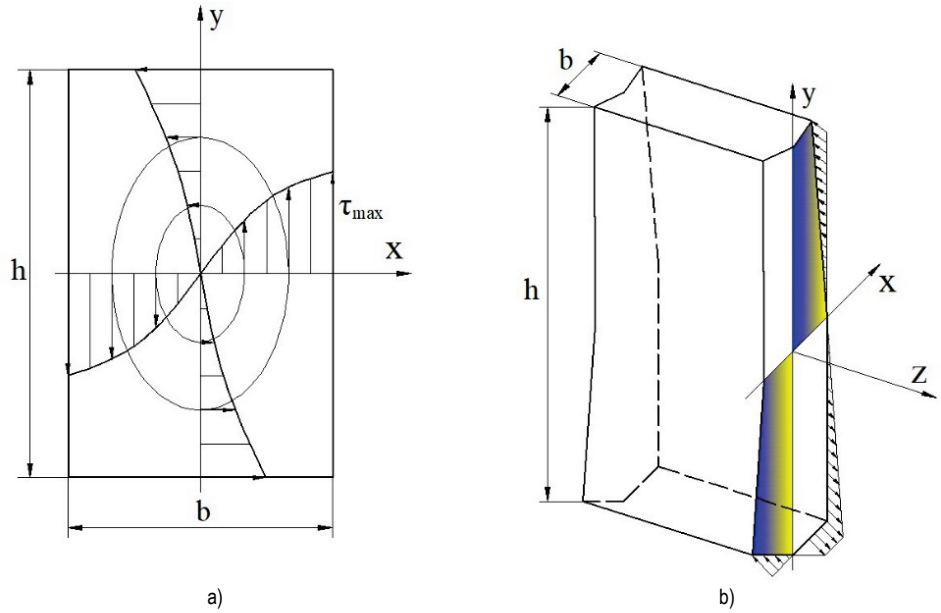

Figure 2 a) Torsion stress distribution over rectangular cross-section; b) Deformed narrow rectangular cross-section at $h >> b$

The distribution of tangential stress across rectangular cross-section of bar is shown in Fig. 2a.

The maximum torsional stress τ_{max} appears on the surface at the closest point to the centre of the longer side. The ellipse inside cross-section in Fig. 2a, presents the stress curves. The highest displacement occurred at the corners of rectangular cross sections as schematically shown in Fig. 2b. In our case, the cross-section of torsion bar consists of very narrow laminae and it is considered that $h/b > 7$.

Generally, the harmonic function takes the value 0 or $\psi(x,y) = 0$, and the windup function is much simplified, as follows:

$$\Phi(x,y)=\frac{\mathrm{C}}{2}\cdot\left[x^2-\frac{b^2}{4}\right] \text{ for } h>>b \tag{4}$$

By solving differential Eq. (1), we simply derive expressions to determine the maximum torsional stress and torsional twist of the narrow prismatic bar in the following form:

$$T=\mathrm{C}\cdot\int_A\left[x^2-\frac{b^2}{4}\right]\cdot\mathrm{d}x\cdot\mathrm{d}y=-\mathrm{C}\cdot b^3\cdot\frac{h}{6}\rightarrow\mathrm{C}=-\frac{6\cdot T}{h\cdot b^3} \tag{5a}$$

$$\tau_{xy}=0,\ \tau_{zy}=\tau=-\mathrm{C}\cdot x=\frac{6\cdot T\cdot x}{h\cdot b^3}\rightarrow\ \tau_{\max}=\frac{3\cdot T}{h\cdot b^2};x=\pm\frac{b}{2} \tag{5b}$$

$$\vartheta'=-\frac{\mathrm{C}}{2\cdot G}=\frac{3\cdot T}{G\cdot h\cdot b^3}\rightarrow\ \tau_{\max}=G\cdot b\cdot\vartheta' \tag{5c}$$

$$k_T=\frac{T}{\vartheta}=\frac{b^3\cdot h\cdot G}{3\cdot L} \tag{5d}$$

$$I_p=\frac{b\cdot h}{12}\cdot\left[b^2+h^2\right] \tag{5e}$$

In Eqs. (5a) to (5e) the symbols have the following meanings:

τ, $\tau_{\max}$	torsion stress / MPa
G	shear modulus / MPa
T	torque / Nmm
ϑ'	windup angle normalized by length L / rad/mm
w	deflection of cross section in z direction / mm
k_T	torsion spring rate / Nmm/rad
I_p	polar moment of inertia / mm^4

3 MECHANICAL PROPERTIES OF TESTED LAMINATED TORSION BARS

Laminated torsion bars were made of spring steel with Young's modulus E = 205 GPa, shear modulus G = 80000 MPa, Poisson's ratio v = 0,3 and tensile yield strength $R_{p0,2}$ = 1450 MPa, tensile strength R_m =1560 MPa, and shear yield strength τ_e = 660 MPa. Dimensions of the spring lamella were: length L = 350 mm, width h = 20 mm, thickness b = 2,8 mm (cross section ratio h/b = 7,14, polar moment of inertia I_p =1903,25 mm^4 and windup stiffness ratio I_p/L = 5,44 mm^3) and number of laminae varied from n = 1 to 9. During torsion tests, torque T and windup angle ϑ were measured and recorded. Torsion tests were performed with different numbers of laminae in the bar. As a result of test the torque moment as a function of windup angle, and number of laminae, is given.

4 EXPERIMENTAL DETERMINATIONS OF SPRING CHARACTERISTICS AND RESULTS

Fig. 3a shows the device setup for torsion bar testing. Device was equipped with a torque sensor and a windup angle sensor with HBM electronic data acquisition system CATMAN. Required torque is induced by hand via the gear box, as shown in Fig. 3a. Test was carried out by measuring the torque at windup angles from 0° to 25°, 45° and 57° for the number of laminae in bars from 1 to 9. Ends of the tested laminated bars were clamped by two clamp jaws. There are three different clamping types possible for a laminated torsion bar:

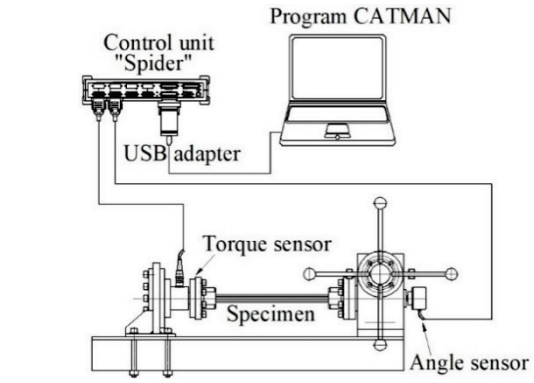

(a)

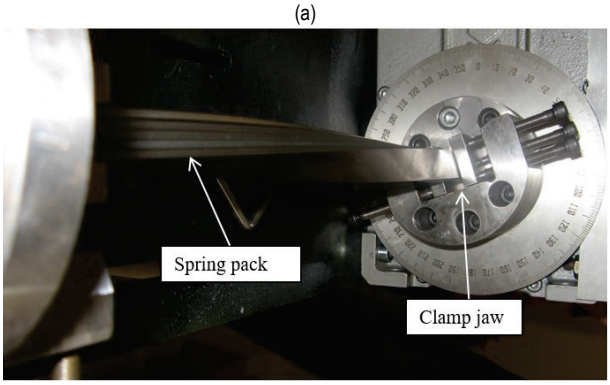

(b)

Figure 3 a) Device for torsion bar testing; b) a bar with five laminae in twisted position

Laminated torsion bar was fully clamped at both sides of the pack. Here an axial movement of the laminae inside the clamp jaw was not possible. Laminae are compressed together, and there is not any spacing between them to allow relative movement.

Laminated torsion bar was clamped on one side by the jaw, and released at the other side. Here released means that the jaw is not fully fastened and allows for relative movement of the laminae in z-direction as shown in Fig. 2b. Laminae are lubricated to reduce the friction between them in case of relative movement. To achieve the relative movement, at least the minimum spacing between laminae is necessary.

Laminated torsion bar was releases and lubricated at both sides in order to allow relative movement in z-direction.

Torque T can be simply obtained from Eq. (5c):

$$T=n\cdot\frac{G\cdot h\cdot b^3}{3}\cdot\vartheta'=n\cdot k_T\cdot\vartheta'=T_{\text{anal}} \tag{6}$$

In Eq. (6) k_T is a torsional constant of the spring package, and n is the number of laminae in the torsion bar. A coefficient between the measured and analytical torque according to Eq. (6), represents the correction coefficient of clamping ξ:

$$\xi=\frac{T_{\text{meas}}}{T_{\text{anal}}} \tag{7}$$

Therefore, actual torque can be calculated by:

$$T_{meas} = \xi \cdot n \cdot k_T \cdot \vartheta' \quad (8)$$

Clamping coefficient ξ takes into account torque. Therefore, the analytical torque should be multiplied by the clamping coefficient ξ to achieve a comparable result with experimental data, Eq. (8). Clamping coefficient ξ is considered as a function of the windup angle ϑ in the torsion direction, and the number of laminae n in the same spring bar. Fig. 4 presents the calculated and measured characteristics of the spring package of the 1, 2, and 9 laminae in the at both sides released package. Fig. 4 shows differences between the theoretical (analytical) and the experimental measured torsion rate. The difference between analytical and experimental results is increasing with numbers of laminae (e.g. 9) while in case of one single laminae bar the agreement is better.

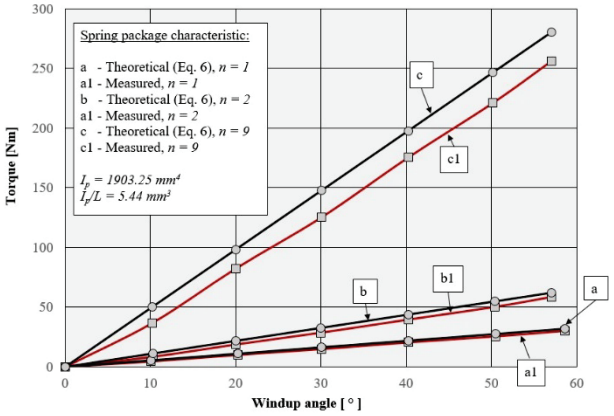

Figure 4 Calculated and measured characteristic of the spring packages of 1, 2, and 9 laminae in the package at both sides released clamping

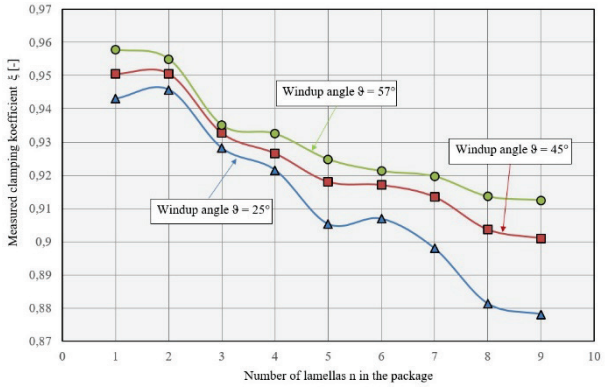

Figure 5 Ratio between measured and analytically obtained torque for same windup angle with different numbers of laminae in torsion for completely released ends of laminated torsion bar

Fig. 5 shows a ratio between the measured and analytically obtained torque for same windup angle with different numbers of laminae in torsion. It is obvious that with a higher number of laminae the difference between the measured and theoretically obtained torque becomes more significant. However, in any case the measured torque is always lower than the theoretically calculated one. Differences become smaller with an increasing windup angle, because the pressure between laminae makes the laminated torsion bar more compact than in the case of low windup angle.

Clamping coefficient can be calculated by means of Eq. (9), where C_{1n}, C_{2n} and C_{3n} are the square equation coefficients and ϑ is the twist angle of the spring package in degrees. Tabs. 1, 2 and 3 show the coefficients of the second order equations for the case of a fully clamped, one side released and fully released spring package.

$$\xi = C_{1n} \cdot \vartheta 2 + C_{2n} \cdot \vartheta + C_{3n} \quad (9)$$

Clamping coefficient can be calculated by means of Eq. (9), where C_{1n}, C_{2n} and C_{3n} are the square equation coefficients and ϑ is the twist angle of the spring package in degrees.

Table 1 Coefficients of quadratic parabola for determination of the clamping coefficient ξ for example of both sides clamped spring pack for ratios h/b = 7,14 and I_p/L = 5,44 mm³

n	C_{1n}	C_{2n}	C_{3n}
1	0,00001692	−0,00158989	1,01896796
2	0,00001760	−0,00172229	1,02435468
3	0,00001828	−0,00185468	1,02974140
4	0,00001895	−0,00198708	1,03512812
5	0,000019635	−0,00211947	1,04051484
6	0,000020312	−0,00225187	1,04590156
7	0,000020989	−0,00238427	1,05128828
8	0,000021666	−0,00251666	1,05674999
9	0,000022343	−0,00264906	1,06206171
10	0,00002302	−0,00278145	1,06744837
11	0,00002369	−0,00291385	1,07283515
12	0,00002437	−0,00304625	1,07822187

Table 2 Coefficients of quadratic parabola for determination of the the clamping coefficient ξ for example of one side released spring pack for ratios h/b = 7,14 and I_p/L = 5,44 mm³

n	C_{1n}	C_{2n}	C_{3n}
1	0,00002937	−0,00217125	1,00242187
2	0,000023854	−0,001699791	0,989185937
3	0,000018333	−0,001228333	0,975900000
4	0,000012812	−0,000756875	0,962714062
5	0,000007291	−0,000285416	0,949478125
6	0,000001770	0,000186041	0,936242187
7	−0,000003750	0,000657500	0,923006250
8	−0,000009270	0,001128958	0,909770312
9	−0,000014791	0,001600416	0,896534375
10	−0,000020312	0,002071875	0,883298437
11	−0,000025833	0,002543333	0,870062500
12	−0,000031354	0,003014791	0,856826562

Table 3 Coefficients of quadratic parabola for determination of the clamping coefficient ξ for example of both sides released spring pack for ratios h/b = 7,14 and I_p/L=5,44 mm³

n	C_{1n}	C_{2n}	C_{3n}
1	−0,00001995	0,00162635	0,91670859
2	−0,00001719	0,00152812	0,90903906
3	−0,00001443	0,00142989	0,90126953
4	−0,00001166	0,00133166	0,89370000
5	−0,00000890	0,00123344	0,88603047
6	−0,00000614	0,00113521	0,87836094
7	−0,00000338	0,00103698	0,87069141
8	−0,00000062	0,00093875	0,86302187
9	0,00000213	0,00084052	0,85535234
10	0,00000489	0,00074229	0,84768281
11	0,00000766	0,00064406	0,84001328
12	0,00001042	0,00054583	0,83234375

Tabs. 1, 2 and 3 show the coefficients of the quadratic parabola for determination of the clamping coefficient ξ.

Figs. 6, 7 and 8 show clamping coefficients ξ for different clamping of spring packs.

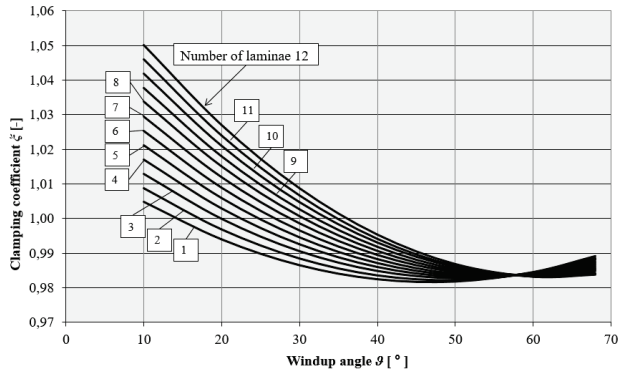

Figure 6 Clamping coefficient ξ for two side fully clamped spring pack for individual laminae with a cross-section ratio h/b=7.14 and I_p/L=5.44 mm^3

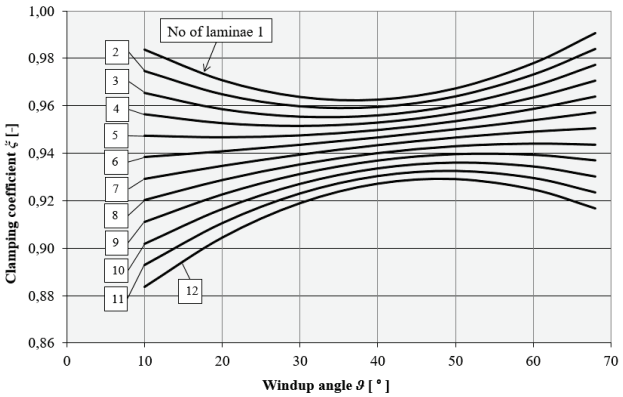

Figure 7 Clamping coefficient ξ for one side fixed and another side with possible relative movement of the torsion bar end for individual laminae with a cross-section ratio h/b = 7,14 and I_p/L = 5,44 mm^3

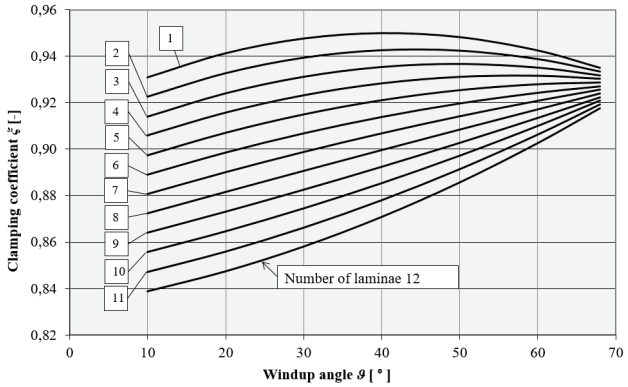

Figure 8 Clamping coefficient ξ for both side released spring packs with an individual laminae cross-section ratio h/b = 7,14 and I_p/L = 5,44 mm^3

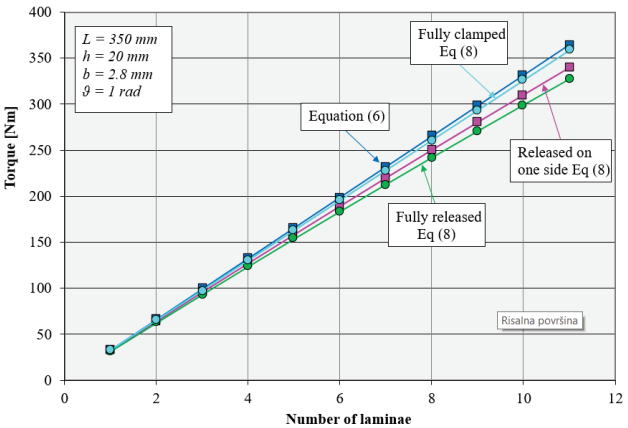

Figure 9 Calculated torque in dependence of number of laminae in the spring package subjected to a windup angle θ = 57,3° (1 rad) and with ratios h/b = 7,14 and I_p/L = 5,44 mm^3

Fig. 9 shows the differences in the torque calculated by using the clamping coefficient for a laminated torsion bar with a different number of laminae. The fully clamped loading torsion bar shows good agreement with theoretical values (Eq. (6)), while the laminated torsion bar with released clamp shows lower torque values. A laminated torsion bar is used for loading and unloading in alternative windup angle cycles. Therefore, in practice it is important to determine a stable torsion rate not only for one loading direction. Fig. 9 shows that for practical reasons, it is necessary to use at least one side released end of a laminated torsion bar. However, all loading torsion rates are linear with the number of laminae in torsion bar.

5 FEM ANALYSIS OF THE LAMINATED SPRING PACKAGE

For comparison, FEM analysis of a spring package with the same geometry and material properties was performed using the ABAQUS computer program. The material properties in the model are the same as given and described in chapter 3. The cubic finite elements C3D8 were used. A nonlinear analysis of the contact boundary problem between the lamellae was carried out. A non−linear analysis required 2334 incremental steps. The spring package is released on each clamp side, so that relative movement of the lamellae is possible. Between each two neighboring lamellas the contact interaction was defined by defining two-surface contact pair as well as at both ends of spring package for clamping. Surface to surface contact was used with finite sliding formulation. Nodes lying on the slave surface are adjusted to remove overclosure with master surface within the tolerance of 0, 1 mm. Contact type interaction properties are defined with the following options, isotropic with penalty friction formulation and pressure - overclosure hard contact were chosen to describe tangential and normal contact behavior. Friction coefficient is set to 0.1 and the contact surfaces are allowed to open after contact.

Fig. 10 shows displacement in z-directions during torsion loading of laminated spring bar for 20°. One can recognize that the displacement at 20° angle in package of 10 laminae is symmetric in the tension and compression zone of laminae. The highest displacement occurs in the outer laminae, while the smallest displacement in z-direction is in the laminae in the middle of the torsion bar.

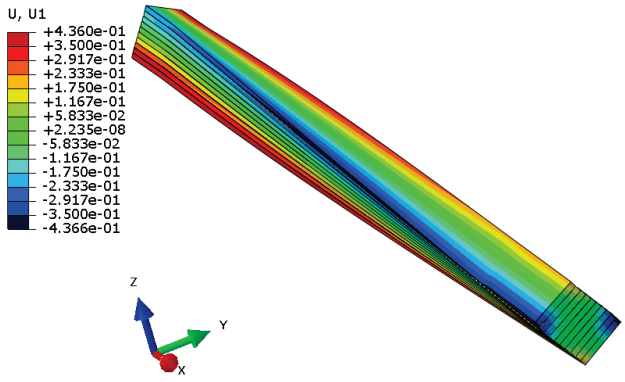

Figure 10 Longitudinal displacement during torsion loading or laminated spring bar for 20° (0,335 rad)

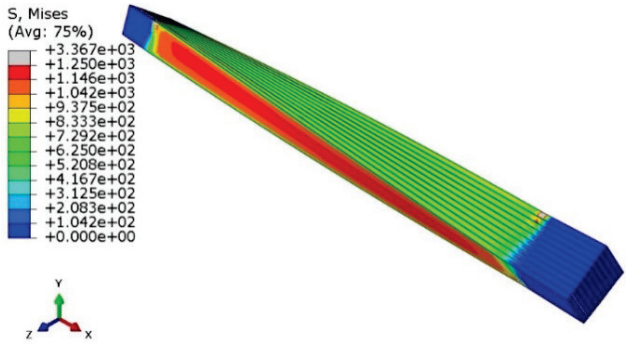

Figure 11 Mises stress distribution at the windup angle of 20° (0,335 rad)

Fig. 11 shows the Von Mises stresses at an angle of rotation of 20°. The maximum von Mises stress achieved is 1250 MPa, but it does not overcome the yield stress of the spring material. Fig. 12 shows the distribution of Von Mises and Tresca stresses along the cross-section at the same angle of rotation. Fig. 12 shows that for both criteria the von Mises and Tresca stress distribution the maximum stresses occurred on the surface of laminae. Fig. 12 shows that all laminae are loaded with the same stress without any influence of their position in the package.

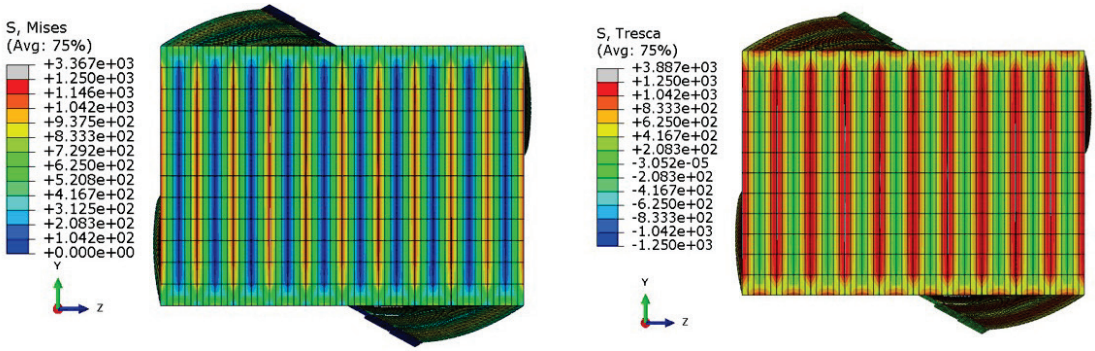

Figure 12 Mises and Tresca stress distribution at the twist angle, of 20°, cross section

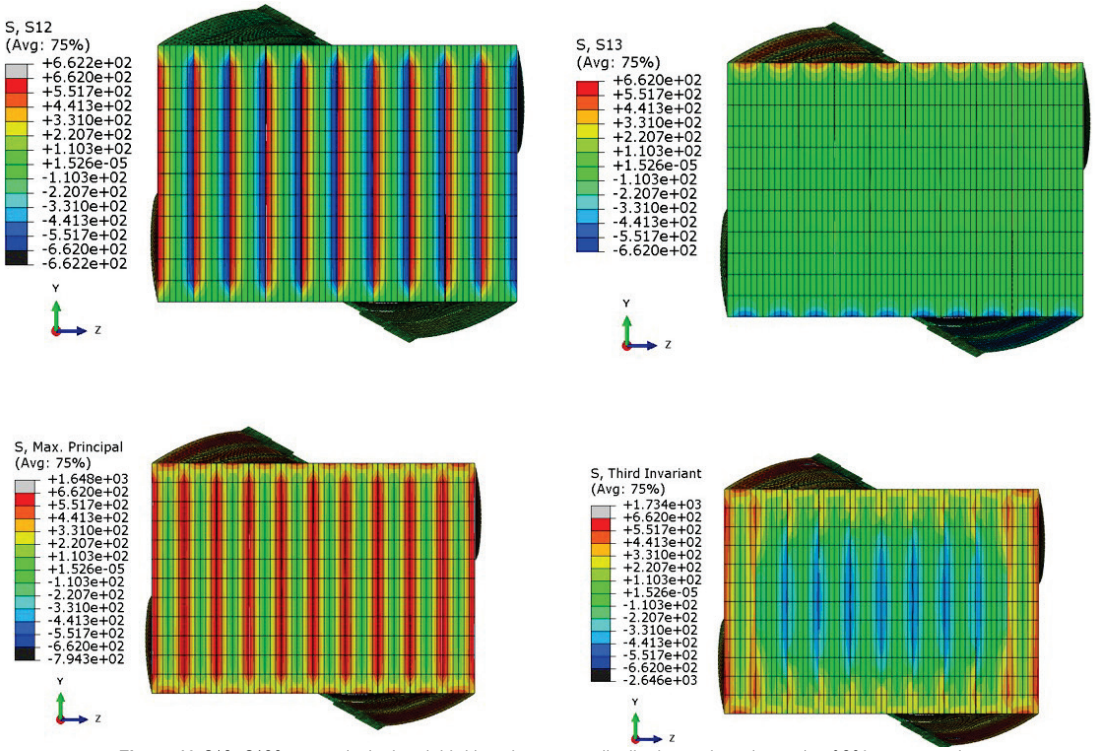

Figure 13 *S*12, *S*123, max principal and third invariant stress distribution at the twist angle of 20°, cross section

Fig. 13 shows the *S*12, *S*13, Max Principal and the Third invariant stress distribution across the cross-section of the Torsion Springs package at a twist angle of 20°. Fig. 13 shows that all laminae in a laminated torsion bar are uniformly loaded with the same stress, and that stress in cross-section of individual laminae does not depend on the distance from the centre of the laminated torsion bar. It confirms the assumption that cumulative torque is possible to calculate by taking into account just the number of laminae as shown given in Eq. (6). Only the third invariant stress shows the highest values at the laminae edge of torsion bar.

Tab. 4 shows a comparison between the FEM and the analytically calculated torsion rate for 1, 2 and 10 laminae in the laminated torsion bar under a constant shear stress introduced by a windup angle of 20° (0,349 rad). It is obvious that the analytical solution obtained by Eq. (7a) and SAE solution without correction for stiffness provide similar results. In the case when correction for stiffness is given by Saint-Venant's function the torsion rate k_T and torque are more than three times smaller.

Table 4 Results for windup angle 20° (0,349 rad) for calculated stress, torsion rate and Torque from FEM, Analitical solutions and SAE compendium, respectively

	shear stress / MPa		torsion rate k_T / Nm/rad			Torque / N·m	
Laminae No.	FEM	T_{anal} Eq. (5b)	anal. Eq.(7a)	SAE* ($\eta_3 = 1$)	SAE** $\eta_3 = 0{,}305$	T_{anal} Eq. (6)	SAE** $\eta_3 = 0{,}305$
1	662	637	95,3	100,35	30,6	33,27	10,68
2	662	637	190,6	200,70	61,2	66,53	21,37
10	662	637	953,1	1003,52	306,1	332,69	106,84

*$\eta_3 = 0{,}333 - 0{,}2/(h/b) = 0{,}305$

Table 5 Difference in Torque / Nm caused by different clamping manner for same windup angle 20°

	Torque / N·m	both clamping	one fixed	both realised			
Laminae No.	T_{anal} Eq. (6)	T_{meas}	T_{meas}	T_{meas}	T_{FEM}		
1	33,27	33,89	33,33	30,52	32,5	6,09%	measured
10	332,69	354,86	294,13	282,13	323,4	12,76%	assumed

Tab. 5 shows good agreement between the numerically and experimentally measured torque for a single laminae torsion bar. With a released end of the laminated torsion bar the torque decreases and the difference became higher with a larger number of laminae in the laminated spring bar. However, the laminated torsion bar with both released ends provides repeatability of torsion rate and therefore the corrected torque is relevant for the laminated torsion bar.

6 CONCLUSIONS

The obtained results show good agreement between numerically and experimentally measured torque for a single lamina torsion bar. With a released end of the laminated torsion bar the torque decreases and the difference became higher with a larger number of laminae in the laminated spring bar. In order to obtain repeatability of torsion rates at least one end of the laminated torsion bar should be released. The measured torsion rate is lower than the theoretically calculated one, but actually experimental behaviour is relevant for alternative torsion loading. The correction coefficients are calculated as the ratio between the measured torque and the analytically determined torque. The correction coefficients are different with respect to the manner of clamping the laminated torsion bar. Experimental and numerical results show that Saint-Venant's coefficients in SAE are valid for an aspect ratio h/b between 2 to 7 for stiffness corrections, but are not appropriate for calculating the torsion rate where the width to thickness ratio exceeds $h/b > 7$.

Acknowledgements

The authors would like to acknowledge ARRS (Slovenian Research Agency) for the support provided during this research within the frame of research program P2-0137.

7 REFERENCES

[1] SAE International: Manual on Design and Manufacture of Torsion Bar Springs and Stabilizer bars, 2000 Edition HS-796: Society for Automotive Engineering Inc. Warendale Pa. ISBN 0-7680-0629-5

[2] Swanson, R. S. (1998). Torsion of laminated rectangular rods. *Composite Structures, 42*, 23-31. https://doi.org/10.1016/S0263-8223(98)00055-5

[3] Danao, L. A. M. & Cabrera, M. R. (2007). Torsion of a Rectangular Prismatic Bar: Solution Using a Power Fit Model. *Philippine Engineering Journal, 28*(1), 77-98.

[4] Francu, J., Novačkova, P., & Janiček, P. (2012). Torsion of a Non-Circual Bar. *Engineering Mechanic, 19*(1), 45-60.

[5] Teimoori, H., Faal, R. T., & Das, R. (2016). Saint-Venant torsion analysis of bars with rectangular cross-section and effective coating layers. *Appl. Math. Mech.-Engl. Ed., 37*(2), 237-252. https://doi.org/10.1007/s10483-016-2028-8

[6] Goodier, J. N. & Timoskenko, S. P. (1970). *Theory of Elasticity*, 3rd ed, McGraw-Hill. https://doi.org/10.1115/1.3408648

[7] Savoia, M. & Tullini, N. (1993). Torsional response of inhomogeneous and multilayered composite beams. *Composite Structures, 25*, 587-594. https://doi.org/10.1016/0263-8223(93)90207-7

[8] Kostrenčić, Z. (1982). *Teorija elastičnosti*, Školska knjiga Zagreb.

[9] Brčić, V. (1982). *Otpornost materijala*, Građevinska knjiga Beograd.

[10] Rašković, D. (1985). *Teorija elastičnosti*, Naučna knjiga Beograd.

[11] Gentiluomo, J. A. (1980). *Design of Laminated Torsion Bar Springs*, Procurement Directorate Watervilient Arsenal, N. Y. 12189, U. S. Army Technical Report, https://doi.org/10.21236/ADA083449

[12] Močilnik, V., Gubeljak, N., & Predan, J. (2011). Model for fatigue lifetime prediction of torsion bars subjected to plastic presetting. *Tehnički vjesnik, 18*(4), 537-546.

[13] Anđelić, N. & Milošević-Mitić, V. (2006). Optimization of a thin-wall cantilever beam at constrained torsion. *Structural Integrity and Life, 6*(3), 121-128.

Contact information:

Vinko MOČILNIK, PhD, Assistant Professor
(Corresponding author)
University of Maribor, Facutly of Mechanical Engineering,
Smetanova 17, 2000 Maribor, Slovenia
E-mail: vinko.mocilnik@siol.net

Jožef PREDAN, PhD, Assoc. Professor
University of Maribor, Facutly of Mechanical Engineering,
Smetanova 17, 2000 Maribor, Slovenia
E-mail: jozef.predan@um.si

Nenad GUBELJAK, PhD, Full Professor
University of Maribor, Facutly of Mechanical Engineering,
Smetanova 17, 2000 Maribor, Slovenia
E-mail: nenad.gubeljak@um.si